NATIONAL ADVISORY COMMITTEE
# FOR AERONAUTICS

TECHNICAL NOTE 3184

BUCKLING OF LONG SQUARE TUBES IN COMBINED COMPRESSION

AND TORSION AND COMPARISON WITH

FLAT-PLATE BUCKLING THEORIES

By Roger W. Peters

Langley Aeronautical Laboratory
Langley Field, Va.

NACA

Washington

May 1954

NATIONAL ADVISORY COMMITTEE FOR AERONAUTICS

TECHNICAL NOTE 3184

BUCKLING OF LONG SQUARE TUBES IN COMBINED COMPRESSION

AND TORSION AND COMPARISON WITH

FLAT-PLATE BUCKLING THEORIES

By Roger W. Peters

SUMMARY

The results of buckling tests of long square tubes loaded in compression, torsion, and combined compression and torsion are compared with theoretical compression and shear buckling curves and with theoretical interaction curves for the buckling of simply supported flat plates. A compression buckling curve previously compared with experiment is again shown to be in good agreement with experimental results; the shear buckling curve derived from compressive stress-strain data by the secant modulus method is in good agreement with experimental results; and theoretical interaction curves previously presented are in good agreement with the results of the combined-load buckling tests. The direction of the loading path is shown to have little or no effect on the shape of the interaction curve.

INTRODUCTION

Extensive theoretical and experimental research has been conducted in order to evaluate the elastic and plastic buckling stresses of flat-plate elements loaded in pure compression (see refs. 1 to 7). The problem of the elastic and plastic buckling of flat-plate elements loaded in pure shear has been treated theoretically and limited experimental data are available to validate these theoretical predictions (see refs. 7 to 10). The problem of the elastic and plastic buckling of flat-plate elements loaded in combined shear and compression also has been treated theoretically (see refs. 11 to 13), but experimental comparison is available for the elastic case only (see ref. 14).

The purpose of this paper is to compare the predictions of the theories for the buckling of long flat plates with the results of elastic and plastic buckling tests on long square tubes loaded in pure compression, pure torsion, and combined compression and torsion.

SYMBOLS

b   width of plate

E   Young's modulus of elasticity

k_c plate buckling coefficient in compression

k_s plate buckling coefficient in shear

L   length of specimen

R_c ratio of compressive stress when buckling occurs under combined
                loading to compressive stress when buckling occurs under
                compression alone

R_s ratio of shear stress when buckling occurs under combined
                loading to shear stress when buckling occurs under shear
                alone

t   thickness of plate

η_c plasticity reduction factor in compression

η_s plasticity reduction factor in shear

ϵ compressive strain

ν Poisson's ratio in elastic region, $\nu = \frac{1}{3}$

σ compressive stress

τ shear stress

Subscripts:

cr   critical buckling stress

cy   compressive yield

TEST SPECIMENS AND TEST PROCEDURE

Test specimens.- The buckling specimens were cut from ten different
sections of drawn square tube of 14S-T6 aluminum alloy having a nominal
wall thickness of 0.156 inch. A sketch of the cross section and a table

of the dimensions of the tubes are presented in figure 1. The nominal thickness of the square tubes used in this investigation is continuous around the corners of the tube, whereas those used in reference 2 had a smaller outside corner radius which added material at the corners of the tube. These tubes also differ from the built-up square tubes used in reference 14 in that they have no corner angles to reduce the wall-to-wall continuity of the buckling nodes. Inasmuch as the measured wall thickness showed a variation, the thicknesses shown in figure 1 are mean thicknesses based on the cross-sectional areas and the nominal widths of the specimens. Measurement of a number of tubes showed the actual width to be the same as the nominal width within the limits of accuracy of measurement. The cross-sectional areas were determined from the weights and measured lengths of the specimens. The nominal length of the specimens was made approximately nine times the cross sectional width to ensure behavior as a long plate. The ends of the specimens were machined flat, square, and parallel. The specimens were bolted to male fixtures consisting of an integral end plate and snug-fitting plugs. Doublers were necessary at the ends of the smaller tubes which buckled at high shear stresses.

Material stress-strain properties.- Compressive stress-strain tests were made on longitudinal single-thickness specimens taken from each of the stock lengths of square-tube material from which the buckling specimens were cut. The average longitudinal compressive stress-strain curve determined from these tests is presented in figure 2. This curve is the average of 182 curves, 90 percent of which fall within a ±5 percent scatter band at the compressive yield stress.

A limited number of compressive and tensile stress-strain tests made on longitudinal and transverse single-thickness specimens taken from one stock length of square-tube material manifested yield strengths which were very nearly identical. This fact plus the results of isotropy tests on similar material reported in reference 2 indicated that extensive isotropy tests were not necessary in this investigation.

Buckling tests.- The buckling tests were made in the combined load testing machine of the Langley structures research laboratory. (See fig. 3.) The buckling loads for the four walls of each tube were determined from autographic load-displacement curves in a manner similar to that described in reference 2. The buckling load for each specimen was taken as the average of the buckling loads for the four walls.

Pure torsion buckling tests were made on specimens of each size of tube to provide additional experimental verification of the theories for pure shear buckling and to determine the pure shear end points for the experimental interaction curves. Similarly, pure compression tests were made to determine the pure compression end points.

The combined compression and torsion tests were made along the three typical loading paths shown in figure 4. Loading path A is a radial loading path in which compression and torsion were increased at a fixed ratio in accordance with the assumptions made in reference 12. Loading path B is a rectangular loading path in which a pure compression load was applied to a value less than pure compression buckling and, with this compression value held constant, torsion was applied until buckling occurred. Loading path C is a rectangular loading path in which a pure torsion load was applied to a value less than pure torsion buckling and, with this torsion value held constant, compression was applied until buckling occurred. In the radial loading tests, displacements were recorded autographically with either the compression or torsion load as the abscissa. The load (torsion or compression) not used as the abscissa was recorded as the ordinate to provide an autographic record of the loading path. In the rectangular loading tests, displacements were recorded against that load which was being increased to produce buckling, that is, torsion in loading path B and compression in loading path C.

RESULTS AND DISCUSSION

Pure compression and pure torsion buckling.- The results of the theories for the plastic buckling of flat plates are usually expressed as

$$\sigma_{cr} = \eta_c \frac{k_c \pi^2 E}{12(1 - \nu^2)(b/t)^2}$$

or

$$\tau_{cr} = \eta_s \frac{k_s \pi^2 E}{12(1 - \nu^2)(b/t)^2}$$

in which η_c and η_s, the plasticity reduction factors, are determined from compressive stress-strain properties. Accordingly, the pure compression and pure torsion buckling data are presented in figures 5(a) and 5(b), respectively, by curves of η_c plotted against σ_{cr} and η_s plotted against τ_{cr} which were computed according to several theories of plastic buckling. For the solid-line curves, the plasticity reduction factors were computed in accordance with references 5 and 9 by Stowell.

The dotted-line curves were computed in accordance with reference 7 by Bijlaard. The dashed-line curves were computed by the secant modulus method suggested by Gerard in references 6 and 10.

Comparison of the experimental points for compression buckling of the walls of a square tube with the theoretical curves of the plasticity reduction factor indicates that the theory of reference 5 most nearly predicts the compression buckling of simply supported flat plates.

Comparison of the experimental points for the buckling of the walls of long square tubes loaded in torsion with curves of the shear plasticity reduction factor for simply supported flat plates shows that the results obtained by the secant modulus method presented in reference 10 are in good agreement. In obtaining shear stresses from compressive stresses for presenting the predictions of references 7 and 9, the factor of $\sqrt{3}$ was used as was done in the derivation of the theories presented in those references. For presenting the shear secant modulus method of reference 10, the same relationships as those used in that reference were applied. It should be recognized that the curves of the shear plasticity reduction factor are dependent on the relationship used to determine shear stresses from the compressive stress-strain properties.

Combined compression and torsion buckling.- The results of the combined-load buckling tests are presented in ratio form in figure 6 where they are compared with appropriate theoretical interaction curves. The square tubes represented in figures 6(a) and 6(b) buckle plastically in both pure torsion and pure compression; those represented in figures 6(c) and 6(d) buckle plastically in pure torsion and elastically in pure compression; and those represented in figures 6(e) and 6(f) buckle elastically in both pure torsion and pure compression. For those specimens which buckle plastically the test points are solid; for those which buckle elastically the test points are open. The number of tubes tested to determine the pure compression and pure torsion end points is indicated by the small number adjacent to the end point.

The theoretical interaction curves for the plastic buckling of simply supported flat plates (figs. 6(a) to 6(d)) were plotted from a trial-and-error solution of equations (A13) and (A14) of reference 12. The pure compression and pure torsion end points for these curves were determined by letting the values of torsion and compression equal zero in the solution of the equations in reference 12, equations (A13) and (A14), respectively. The actual values of the stresses computed for the theoretical end points were not necessarily equal to those obtained for the experimental end points. These theoretical interaction curves appear to be slightly conservative when compared with the experimental buckling data for the walls of a square tube.

Also presented in figures 6(a) to 6(d) is the circular arc described by the equation

$$R_c^2 + R_s^2 = 1$$

This circular arc provides a good approximation of the theoretical interaction curve, particularly in the completely plastic buckling case.

A theoretical interaction curve for the elastic buckling of a long square tube was computed by an energy method in reference 13. This interaction curve, derived on the premise that the possible buckling patterns are restricted to those that give continuity of the nodes around the tube, is in excellent agreement with the experimental results of figures 6(e) and 6(f).

Also shown in figures 6(e) and 6(f) is the parabolic interaction curve for the elastic buckling of a single long simply supported flat plate presented in reference 11 and described by the equation

$$R_c + R_s^2 = 1$$

This curve, derived for buckling not restricted by nodal continuity, lies below the test points for the elastic buckling of square tubes.

Comparison of the test points in figure 6 for the three different loading paths reveals that the direction of loading path has very little effect on the shape of the interaction curves.

CONCLUSIONS

Results are presented for the buckling of long 14S-T6 aluminum-alloy square tubes loaded in compression, torsion, and combined compression and torsion. Comparison of these experimental results with theoretically determined compression and shear buckling curves and with theoretically determined interaction curves for long simply supported flat plates warrants the following conclusions:

1. The plasticity reduction factors for the compression buckling of simply supported flat plates derived from compressive stress-strain data according to NACA Rep. 898 are in good agreement with experimental results.

2. The plasticity reduction factors for shear buckling curves derived from compressive stress-strain data in accordance with the secant modulus method are in good agreement with the experimental data.

3. The theoretical interaction curve presented in NACA TN 1751 for the elastic buckling of a long square tube is in excellent agreement with the experimental results.

4. The theoretical interaction curves computed in accordance with NACA TN 1990 for the plastic buckling of long simply supported flat plates are conservative for predicting combined-load buckling of long square tubes.

5. A circular arc provides an adequate interaction curve for combined-load buckling of long square tubes which are completely plastic.
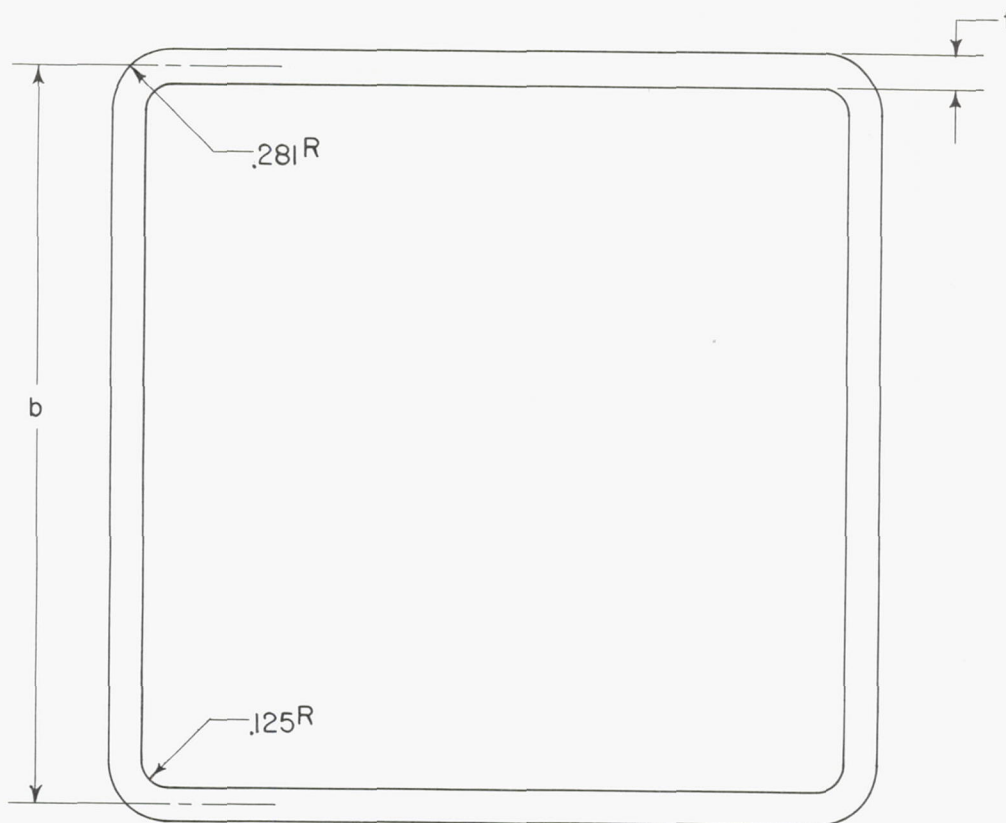
6. The direction of the loading path has little or no effect on the shape of the interaction curves.

Langley Aeronautical Laboratory,
    National Advisory Committee for Aeronautics,
        Langley Field, Va., February 23, 1954.

REFERENCES

1. Stowell, Elbridge Z., Heimerl, George J., Libove, Charles, and
   Lundquist, Eugene E.: Buckling Stresses for Flat Plates and Sections.
   Paper No. 2506, Trans. Am. Soc. Civil Eng., vol. 117, 1952, pp. 545-
   575; Discussion, pp. 576-578.

2. Pride Richard A., and Heimerl, George J.: Plastic Buckling of Simply
   Supported Compressed Plates. NACA TN 1817, 1949.

3. Lundquist, Eugene E., and Stowell, Elbridge Z.: Critical Compressive
   Stress for Flat Rectangular Plates Supported Along All Edges and
   Elastically Restrained Against Rotation Along the Unloaded Edges.
   NACA Rep. 733, 1942. (Supersedes NACA ACR, May 1941.)

4. Heimerl, George J.: Determination of Plate Compressive Strengths.
   NACA TN 1480, 1947.

5. Stowell, Elbridge Z.: A Unified Theory of Plastic Buckling of
   Columns and Plates. NACA Rep. 898, 1948. (Supersedes NACA TN 1556.)

6. Gerard, George: Secant Modulus Method for Determining Plate Insta-
   bility Above the Proportional Limit. Jour. Aero. Sci., vol. 13,
   no. 1, Jan. 1946, pp. 38-44 and 48.

7. Bijlaard, P. P.: Theory and Tests on the Plastic Stability of Plates
   and Shells. Jour. Aero. Sci., vol. 16, no. 9, Sept. 1949,
   pp. 529-541.

8. Stowell, Elbridge Z.: Critical Shear Stress of an Infinitely Long
   Flat Plate With Equal Elastic Restraints Against Rotation Along the
   Parallel Edges. NACA WR L-476, 1943. (Formerly NACA ARR 3K12.)

9. Stowell, Elbridge Z.: Critical Shear Stress of an Infinitely Long
   Plate in the Plastic Region. NACA TN 1681, 1948.

10. Gerard, George: Critical Shear Stress of Plates Above the Proportional
    Limit. Jour. Appl. Mech., vol. 15, no. 1, Mar. 1948, pp. 7-12.

11. Stowell, Elbridge Z., and Schwartz, Edward B.: Critical Stress for
    an Infinitely Long Flat Plate With Elastically Restrained Edges
    Under Combined Shear and Direct Stress. NACA WR L-340, 1943.
    (Formerly NACA ARR 3K13.)

12. Stowell, Elbridge Z.: Plastic Buckling of a Long Flat Plate Under
    Combined Shear and Longitudinal Compression. NACA TN 1990, 1949.

13. Budiansky, Bernard, Stein, Manuel, and Gilbert, Arthur C.: Buckling
      of a Long Square Tube in Torsion and Compression. NACA TN 1751,
      1948.

14. Peters, Roger W.: Buckling Tests of Flat Rectangular Plates Under
      Combined Shear and Longitudinal Compression. NACA TN 1750, 1948.

b	t	$\frac{b}{t}$	L
3.35	0.1535	21.8*	29.0
3.35	.1502	22.3	33.3
3.60	.1533	23.4*	31.0
4.10	.1547	26.4*	35.0
4.35	.1538	28.2	43.1
4.84	.1555	31.2*	42.0
5.34	.1584	33.7	51.1
6.34	.1554	40.7	59.2
7.35	.1530	48.0	69.0
7.85	.1508	52.1	74.1

*Tubes tested in pure torsion only.

Figure 1.- Cross-sectional dimensions of square tubes.
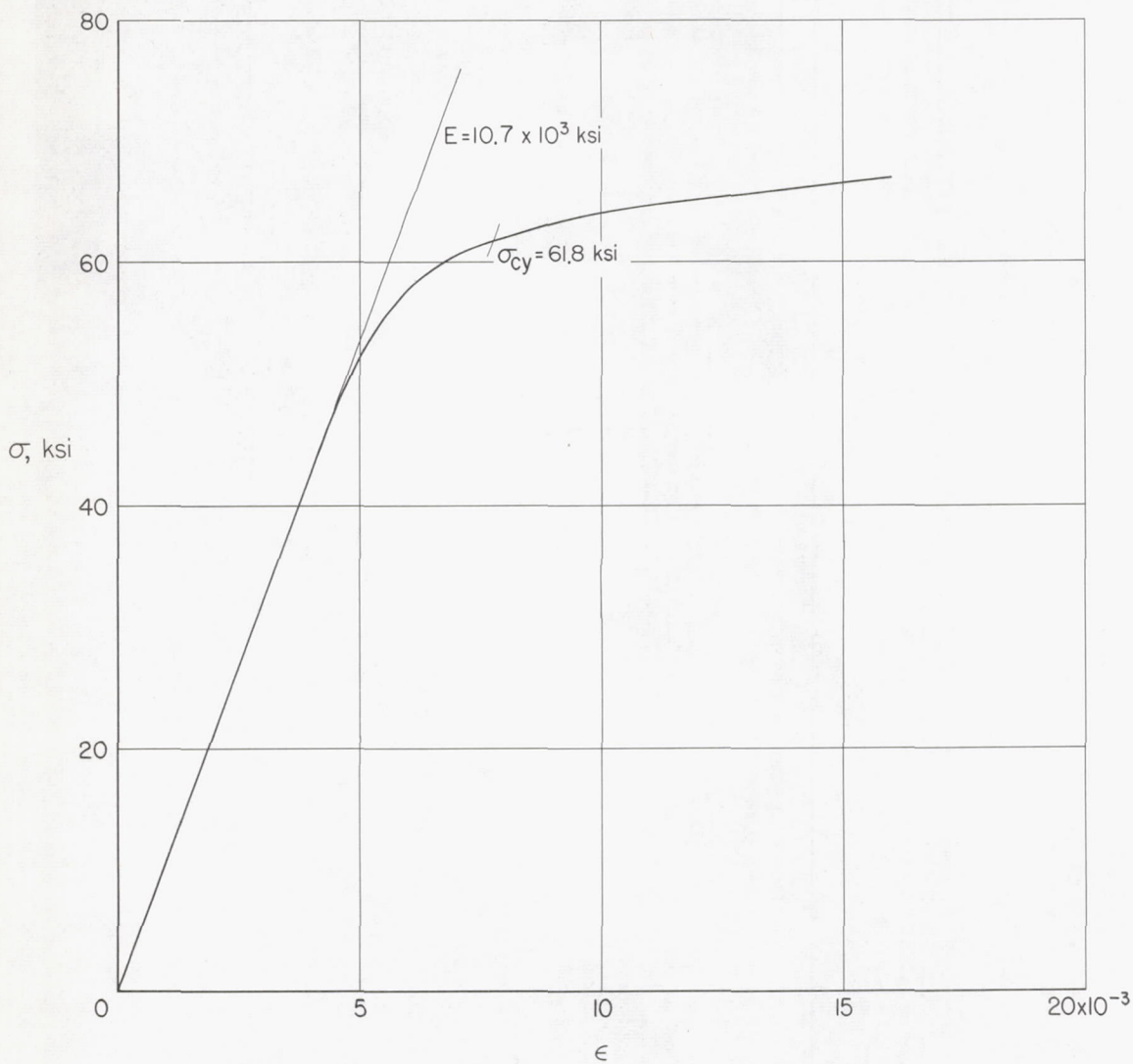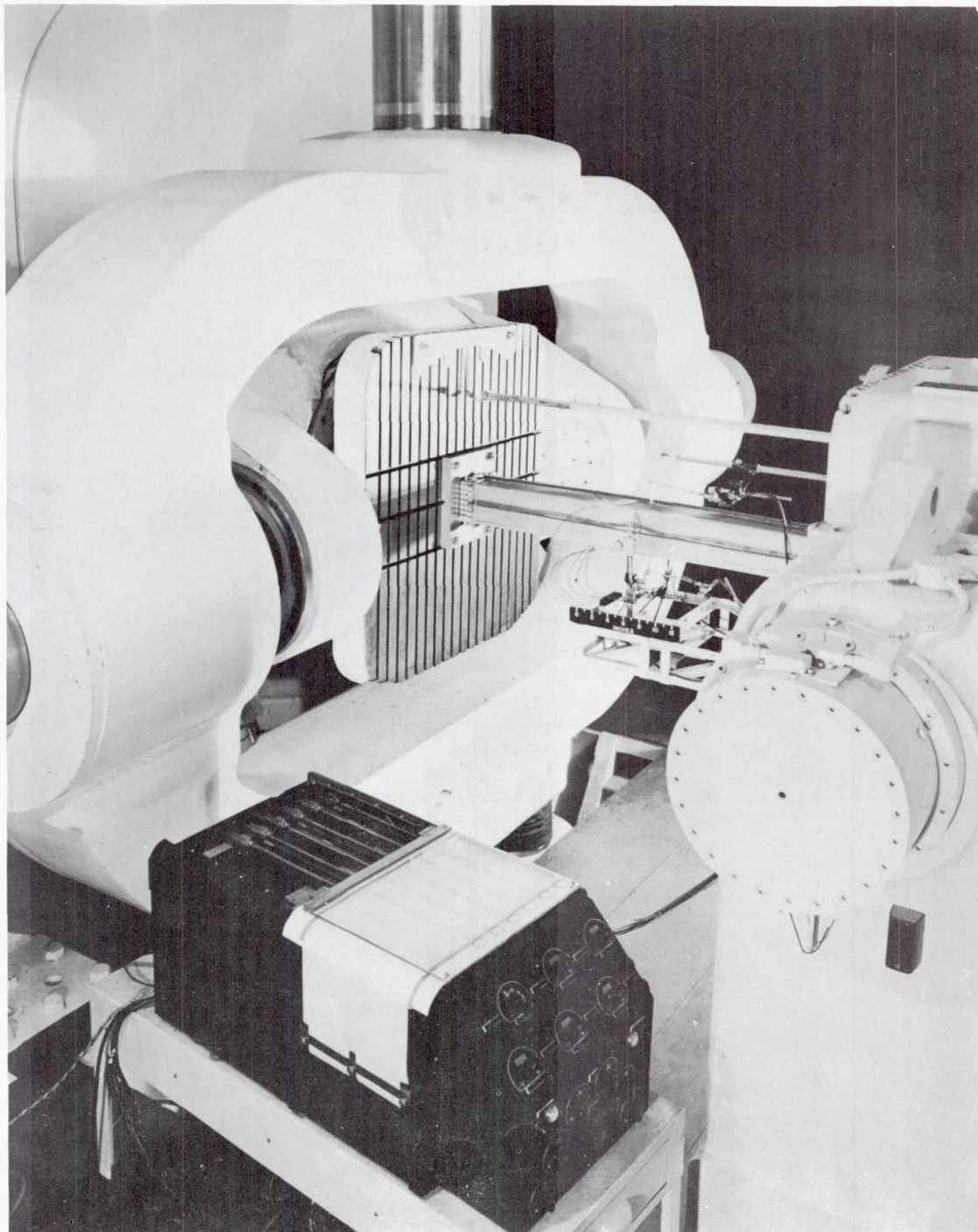
Figure 2.- Average longitudinal compressive stress-strain curve for drawn 14S-T6 aluminum alloy.

L-67355.1

Figure 3.- Test setup in the combined load testing machine of the
Langley structures research laboratory.
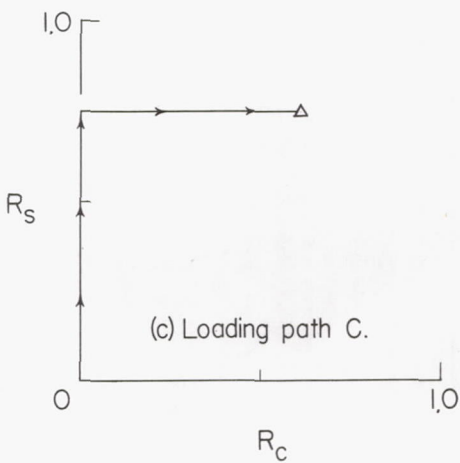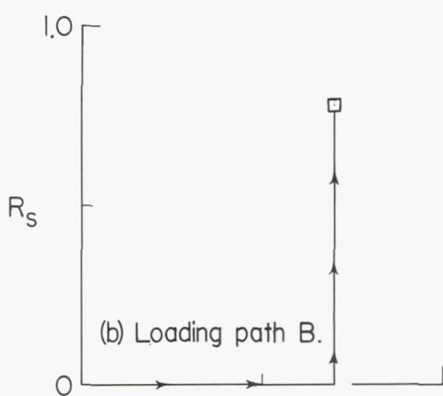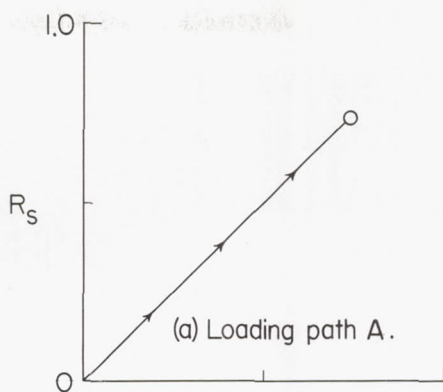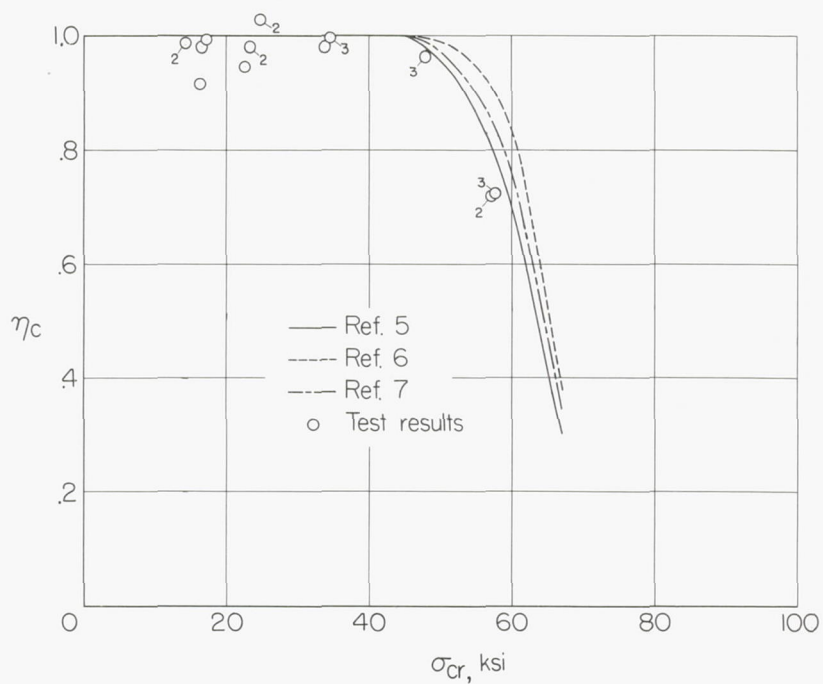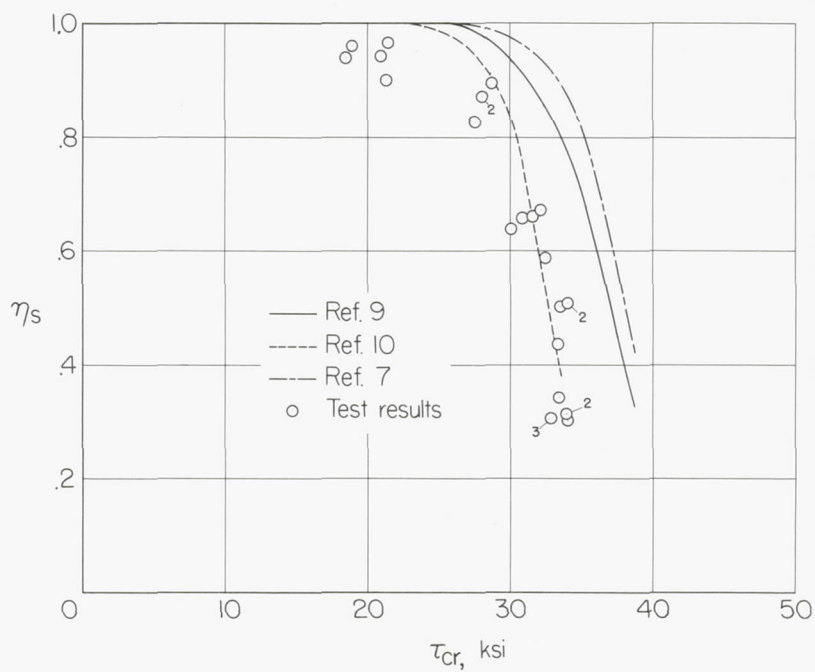
Figure 4.- Typical loading paths for combined compression and torsion buckling tests.

(a) Compression buckling.

(b) Shear buckling.

Figure 5.- Buckling curves for simply supported flat plates of
14S-T6 aluminum alloy.
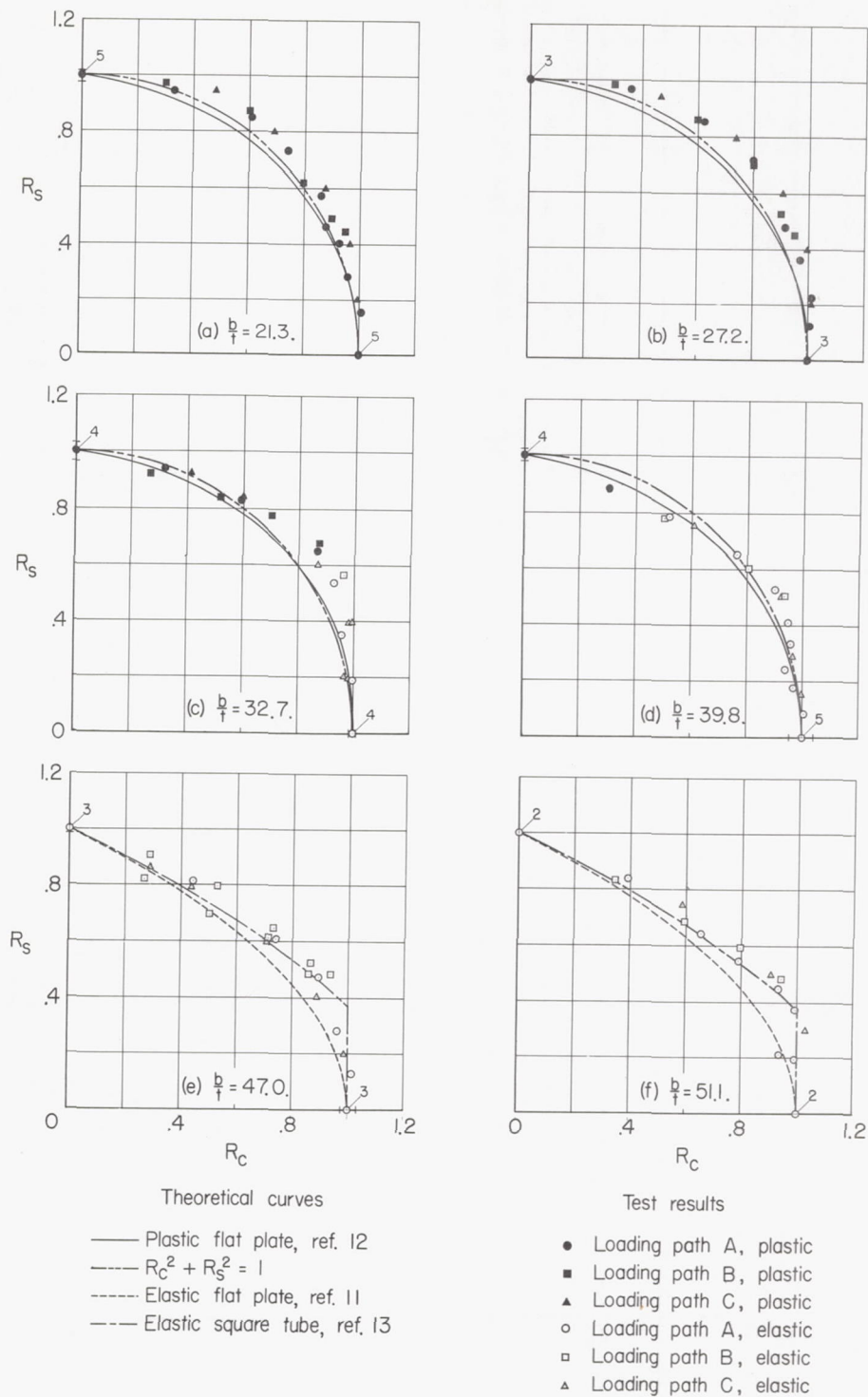
Figure 6.- Interaction curves for the buckling of long simply supported
flat plates of 14S-T6 aluminum alloy under combined shear and
compression loading and long square tubes under combined torsion
and compression loading.